When waves meet vortices: A topological twist in water

Aditya Singh (Experiment), OIST

Jonas Rønning (Theory & Numerics), OIST

Chien-Chia Liu (Experiment), OIST

Anup Kumar (Theory), OIST

Luiza Angheluta (Theory & Numerics)
University of Oslo, Norway

Andres Concha (Theory & Numerics)
Universidad Adolfo Ibáñez, Santiago, Chile

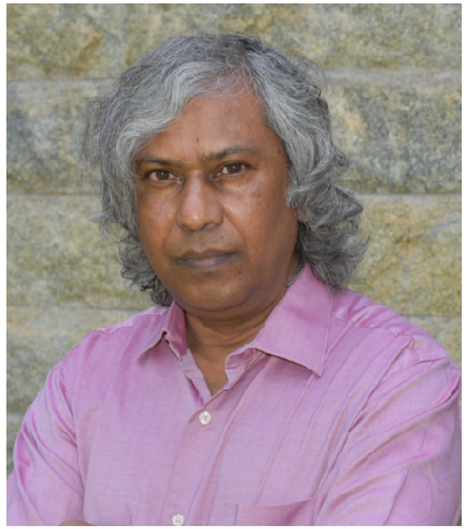

Joseph Samuel (Theory)
ICTS-TIFR, India

MMB (Experiment), OIST

Ehrenberg-Siday-Aharonov-Bohm Effect

Particle with charge q traveling along path P in a region with $\mathbf{B} = 0 \neq \mathbf{A}$ (i.e. $\mathbf{B} = \nabla \times \mathbf{A} = 0$) acquires a phase shift :

$$\frac{q}{\hbar}\int_P \mathbf{A}\cdot d\vec{x}$$

Particles with same start & end pts. traveling along diff. paths acquire phase difference determined by magnetic flux Φ_B:

$$\text{Phase Difference} = \frac{q\Phi_B}{\hbar}. \qquad \Phi_B = \oint \mathbf{A}\cdot d\vec{l}$$

Fields central to observations in classical physics, potentials were deemed a mathematical convenience.

AB effect seemingly contradicted this view; helped clarify the role of gauge potentials in physics.

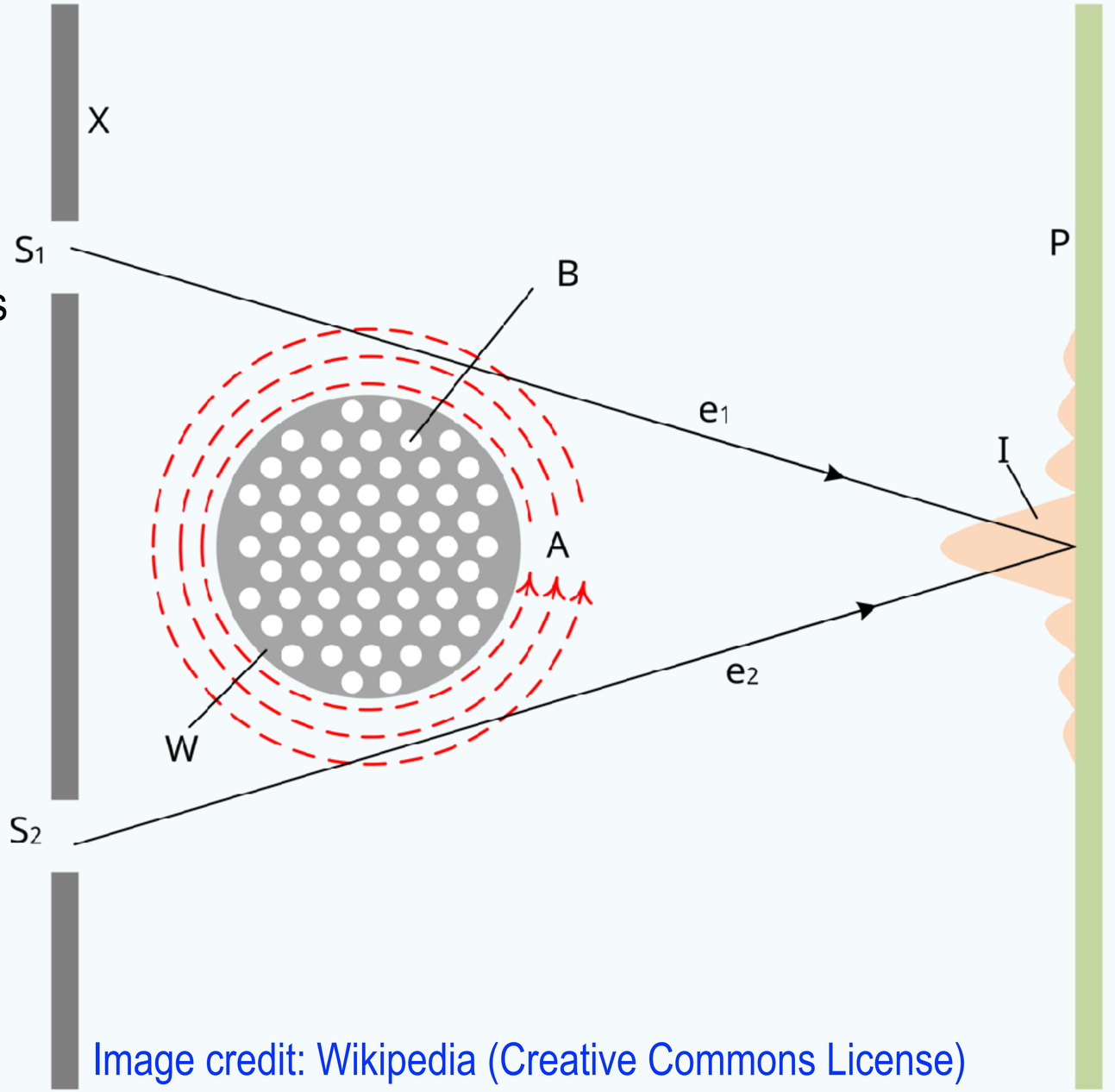

Image credit: Wikipedia (Creative Commons License)

W Ehrenberg and RE Siday, *Proc. Phys. Soc.* **62**, 8 (1949)
Y Aharonov and D Bohm, *Phys. Rev.* **115**, 485 (1959)
A Tonomura *et al, Phys. Rev. Lett.* **56**, 792 (1986)

Wavefront dislocations

AB effect is accompanied by a dislocation in lines of constant phase of the wave function

Wave function: $\psi(\vec{r}) = |\psi(\vec{r})| e^{i\chi(\vec{r})}$

Wavefront: A line where $\chi(\vec{r}) =$ constant

Characterized by $\alpha = \frac{q}{h}\Phi_B$

Dislocation charge is the nearest integer

Not an observable in the quantum regime

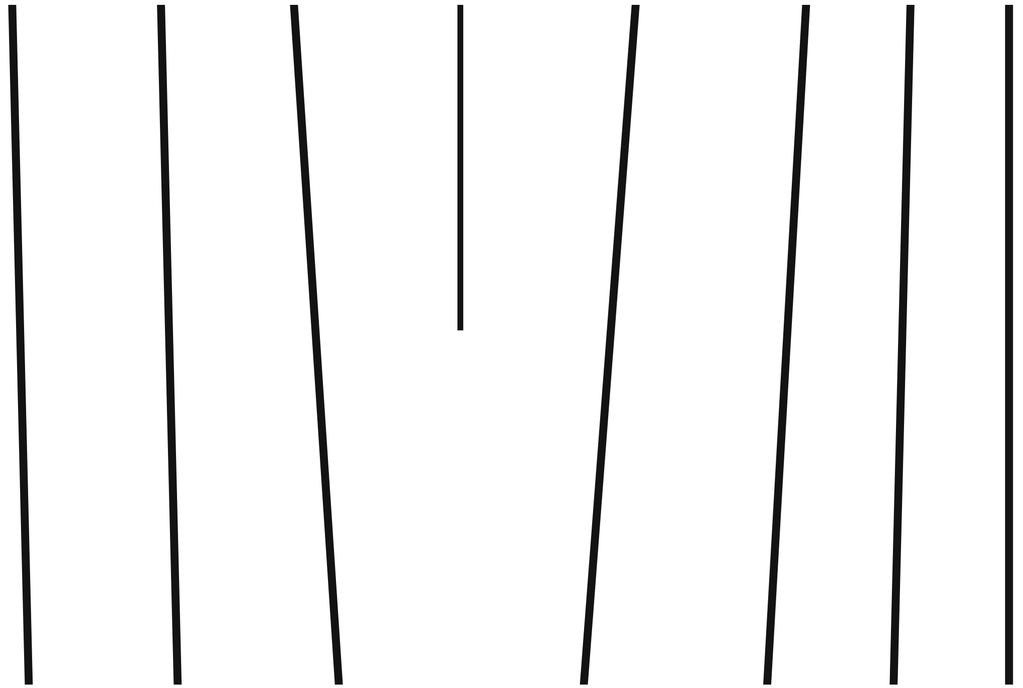

Fluid Analogy

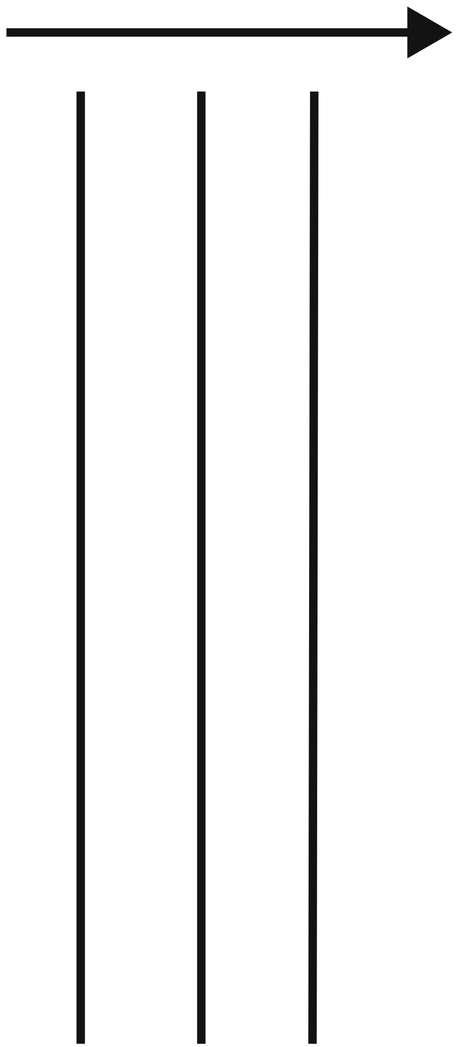

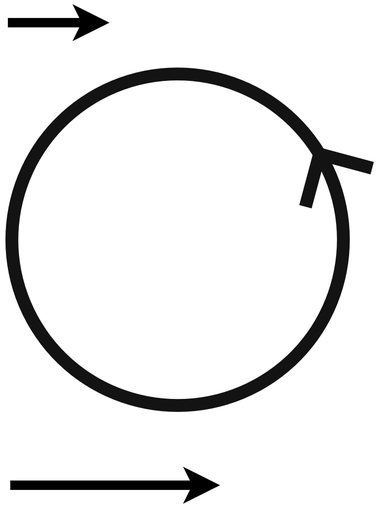

Analog to scattering of waves on an irrotational vortex.

Dislocation parameter: $\alpha_q = \frac{q\Phi_B}{h} \leftrightarrow \alpha_f = -\frac{\Gamma}{\lambda v_g}$

$$\Gamma = \oint d\vec{l} \cdot \mathbf{U}$$

Note: Physical meaning of α

Effect of vector potential similar to that of velocity field

$$\mathbf{A} \leftrightarrow \mathbf{U}$$

$$\mathbf{B} = \nabla \times \mathbf{A} \leftrightarrow \omega = \nabla \times \mathbf{U}$$

JC Maxwell, *Philos. Mag.* **90**, 11 (1861)

Note: Maxwell vs. Helmholtz.

Wavefronts now observable in fluid analogy

Classical water-wave analogue: Prior work

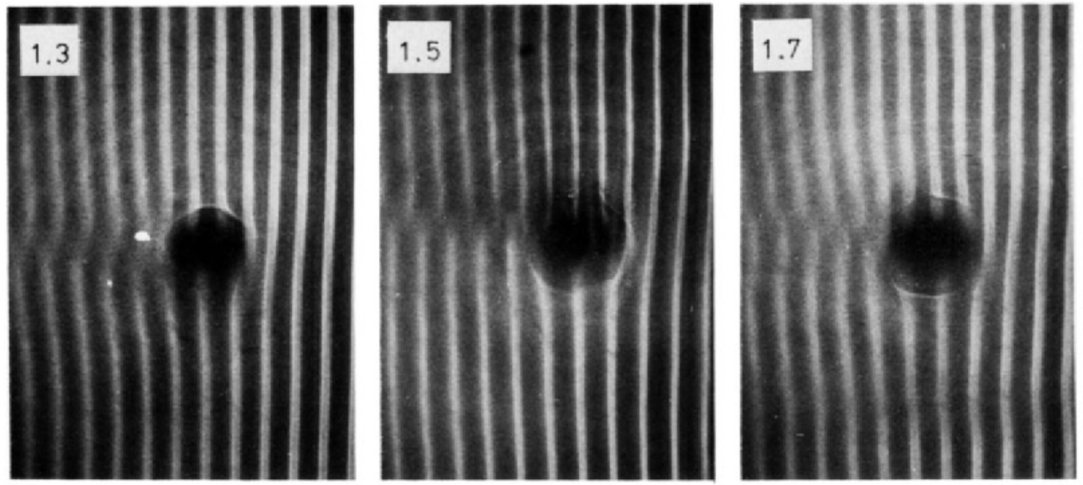

Berry et al. *Eur. J. Phys.* **1**, 154 (1980)

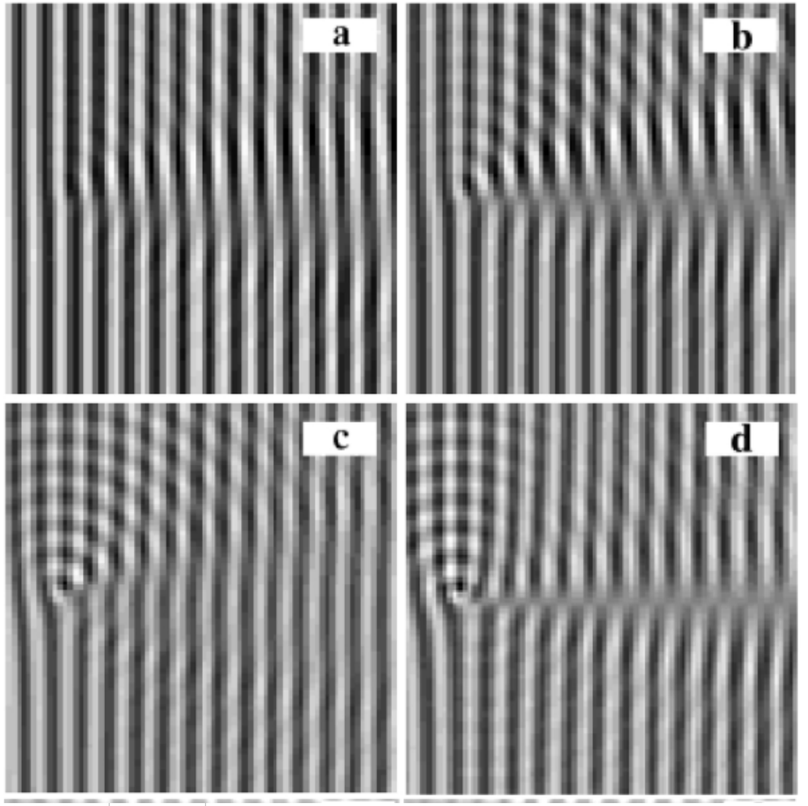

Vivanco & Melo, *Phys. Rev. E.* **69**, 026307 (1999)

The vector potential changes the topology of the far field.
Easily observed from Burgers vector around the vortex.

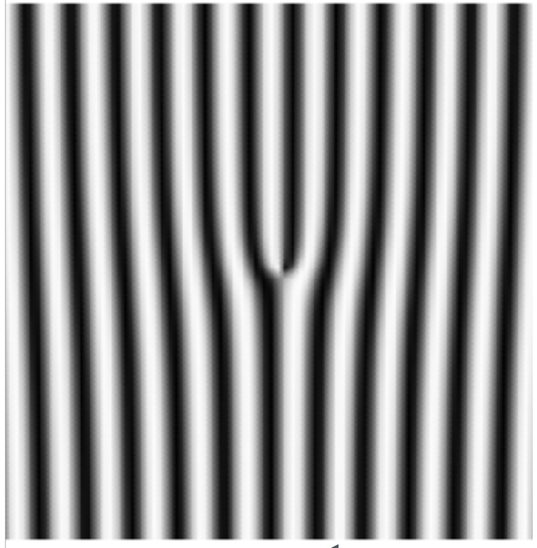

$\alpha = 1$

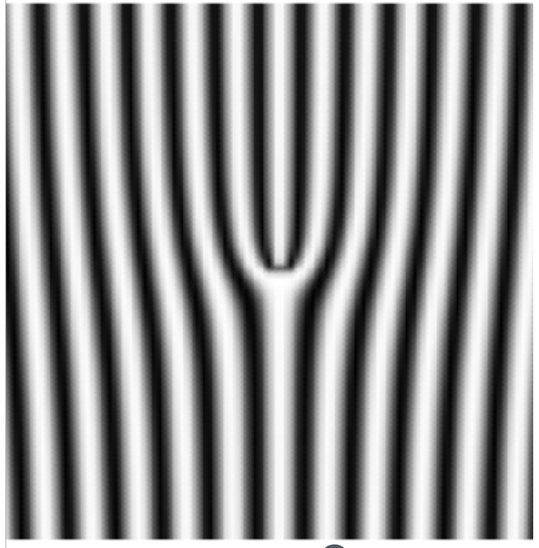

$\alpha = 2$

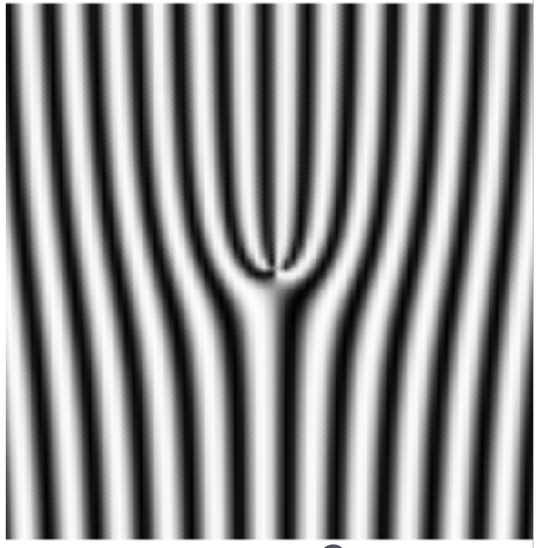

$\alpha = 3$

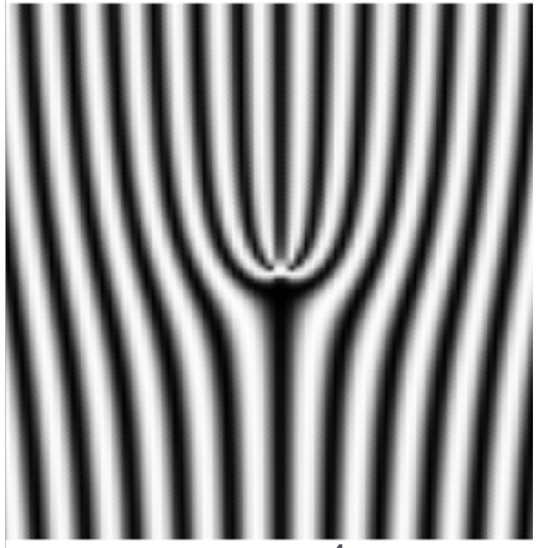

$\alpha = 4$

Simulation at $\alpha = 2$

Prior work: Traveling waves.

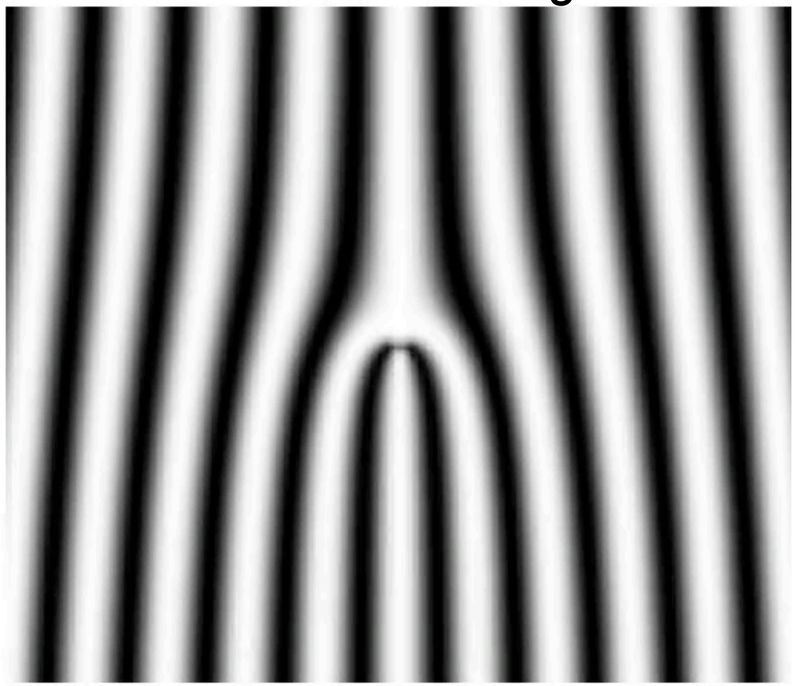

Present study: Standing waves

Classically quantized, rotating, system spanning nodal lines.

This result has not been reported in literature to our knowledge.

We will try to understand it in the remainder of this talk.

$$\frac{1}{2m}\left(-i\hbar\nabla - q\mathbf{A}\right)^2\psi(\vec{r}) = \frac{\hbar^2k^2}{2m}\psi(\vec{r}) \leftrightarrow (\partial_t + \mathbf{U}\cdot\nabla)^2\eta - c^2\nabla^2\eta = 0$$

Schrödinger Equation: Simpler math

Shallow water Equation: Better intuition

η: small surface deformation

$c = \sqrt{gH}$: waves' phase velocity

Background flow $\mathbf{U}(U \ll c)$ induced by vortex irrotational outside vortex core (radius *R*), given by $\mathbf{U} = \frac{\Gamma}{2\pi r}\hat{\varphi}$.

$\hat{\varphi} = [\cos(\varphi), \sin(\varphi)]$: azimuthal unit vector in (x, y) system centered at vortex. Polar angle φ range $(-\pi, \pi]$.

Wave vectors set in $\pm x$ direction $\vec{k} = k\hat{x}$. Surface wave wavelength $\lambda = 2\pi/k \ll R \quad (Rk \ll 1)$.

Irrotational vortex

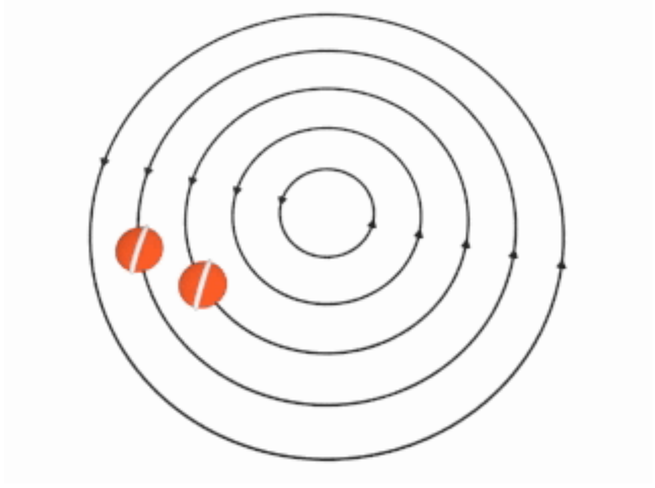

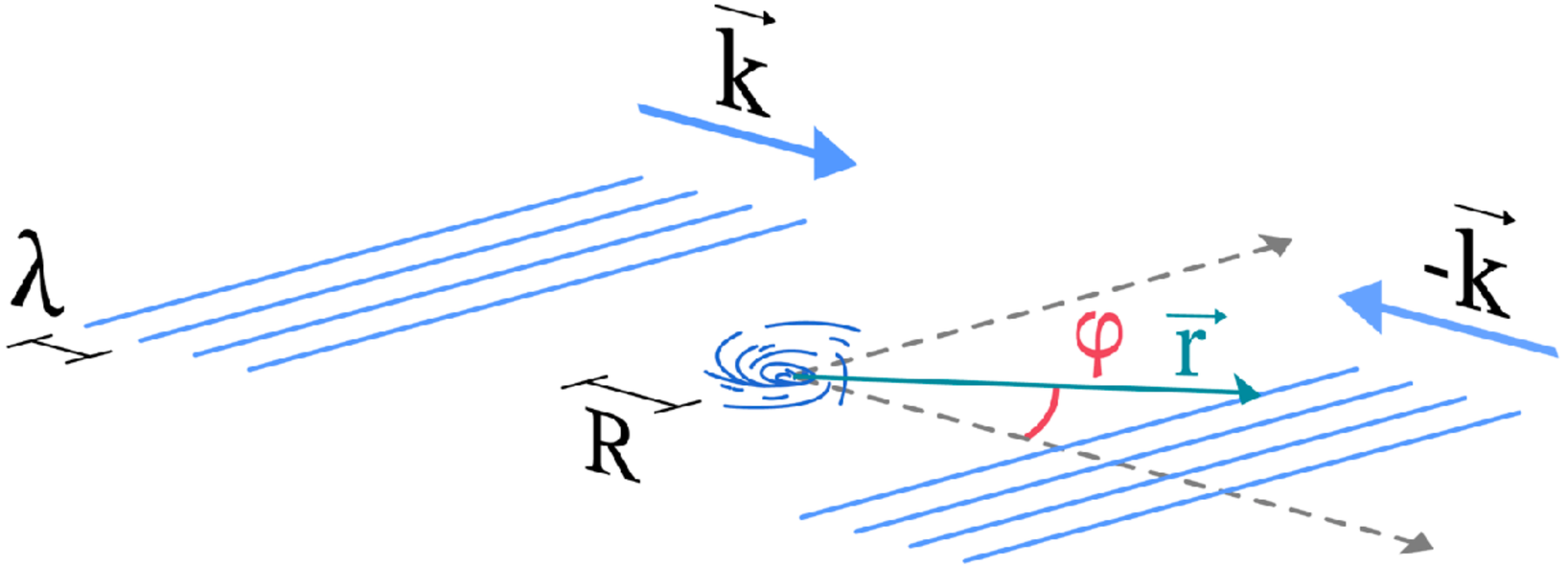

Surface deformation η : $\eta(\vec{r},t) = \mathrm{Re}(e^{-i\nu t}\psi(\vec{r}))$; $\psi(\vec{r})$: travelling wave's complex amplitude.

Adiabatic assumption: vortex velocity **U** and magnetic vector potential **A** small & slowly varying relative to wave function.

Now shallow water eq. maps to Schrödinger eq., and yields far-field correspondence: $\mathbf{U}(\vec{r}) = \frac{\Gamma}{2\pi r}\hat{\varphi} \leftrightarrow \mathbf{A} = \frac{\Phi_B}{2\pi r}\hat{\varphi}$

Berry et al., *Eur. J. Phys.* **1**, 154 (1980). Coste, Lund & Umeki, *Phys. Rev. E.* **60**, 4908 (1999)

Represent standing waves as counter propagating particle beams $\pm\vec{k}$ in $\pm x$-direction. ($\vec{k} = k\hat{x}$)

Express $\psi = \psi_- + \psi_+$; $\psi_\pm$: wave function for scattering of beam with wave vector $\pm k\hat{x}$.

Then $\psi = 2\Sigma_n(-i)^{l_q}J_{l_q}(kr)e^{2ni\varphi}$ for point-like solenoid; J_{l_q}: Bessel function of 1st kind & $l_q = |2n - \alpha|$.

Note: Difference between Berry et al and our treatment is the transformation $n \to 2n$. Has non-trivial consequences.

Numerics: Analytical plots and animations of the amplitude of $\eta(\vec{r},t) = \mathrm{Re}(e^{-i\nu t}\psi(\vec{r}))$ obtained by evaluating the wave function $\psi = 2\Sigma_n(-i)^{l_q}J_{l_q}(kr)e^{2ni\varphi}$ in Python. Summation truncated at n = 200.

A mathematical analogy, *not* an exact correspondence.

- Electron wave function not observable in quantum regime, water wave amplitude is classically observable.
- Phase is not observable in quantum, but classically observable — fact exploited by Berry et al in their 1980 study.
- Quantum case invariant under gauge transformation, but fluid velocity **U** changes by a gradient representing a different physical situation.
- Both systems comparable in particular gauge where $\mathbf{A} \ \& \ \mathbf{U} \propto \frac{(y, -x)}{x^2 + y^2}$. Applies classically if the vortex core is assumed to be negligible. This is the case in the present study.
- "Large gauge transformations" exist in AB system ($\psi \rightarrow e^{(in\varphi)}\psi$) that respect wave function's single valuedness. They change $\alpha \rightarrow \alpha + n$. Not true for water system as such gauge transformations change **U**.

Experimental Design

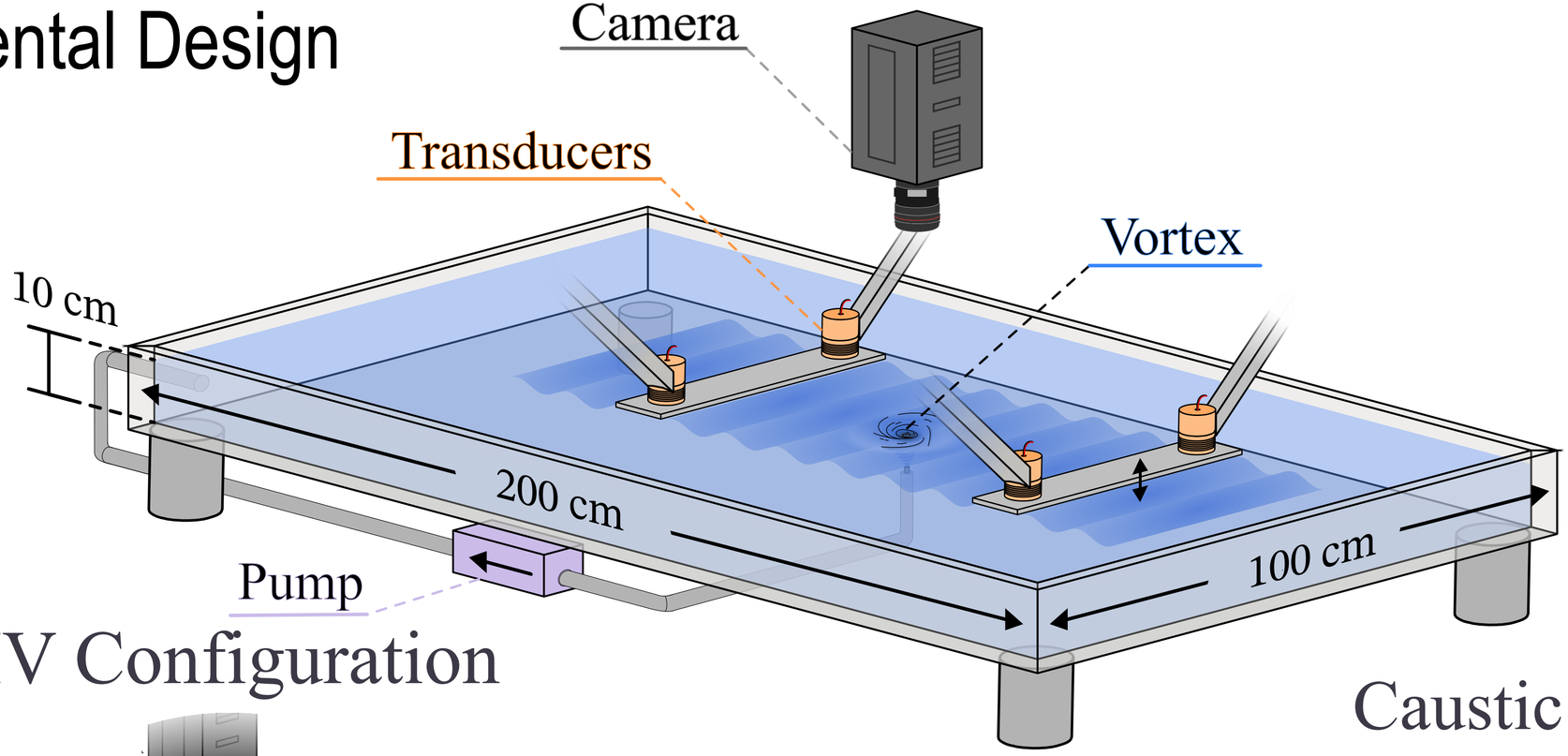

PIV Configuration

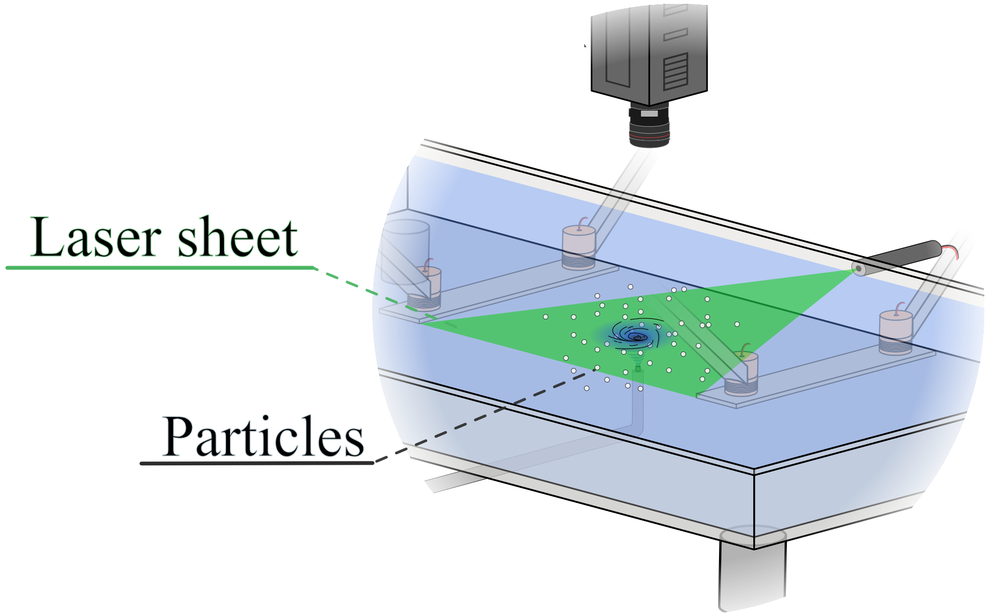

Caustic Configuration

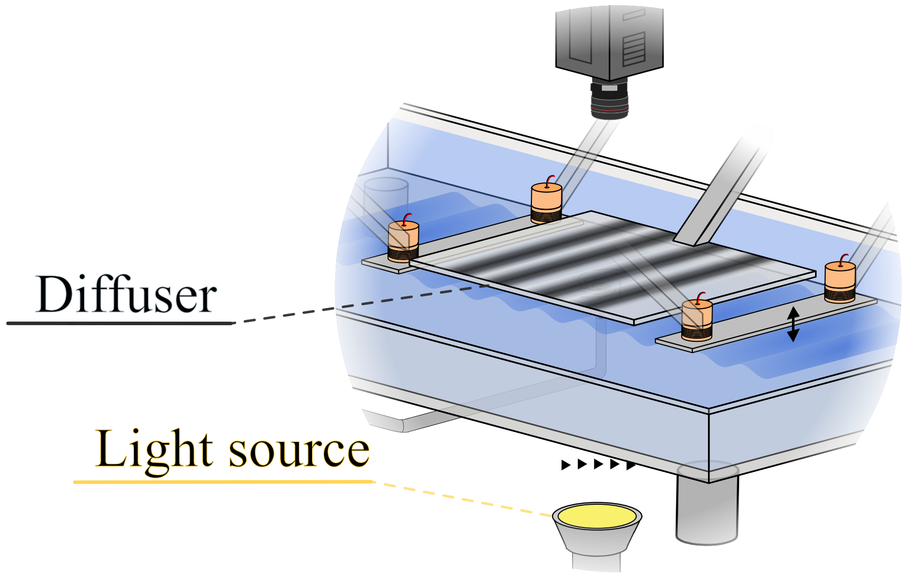

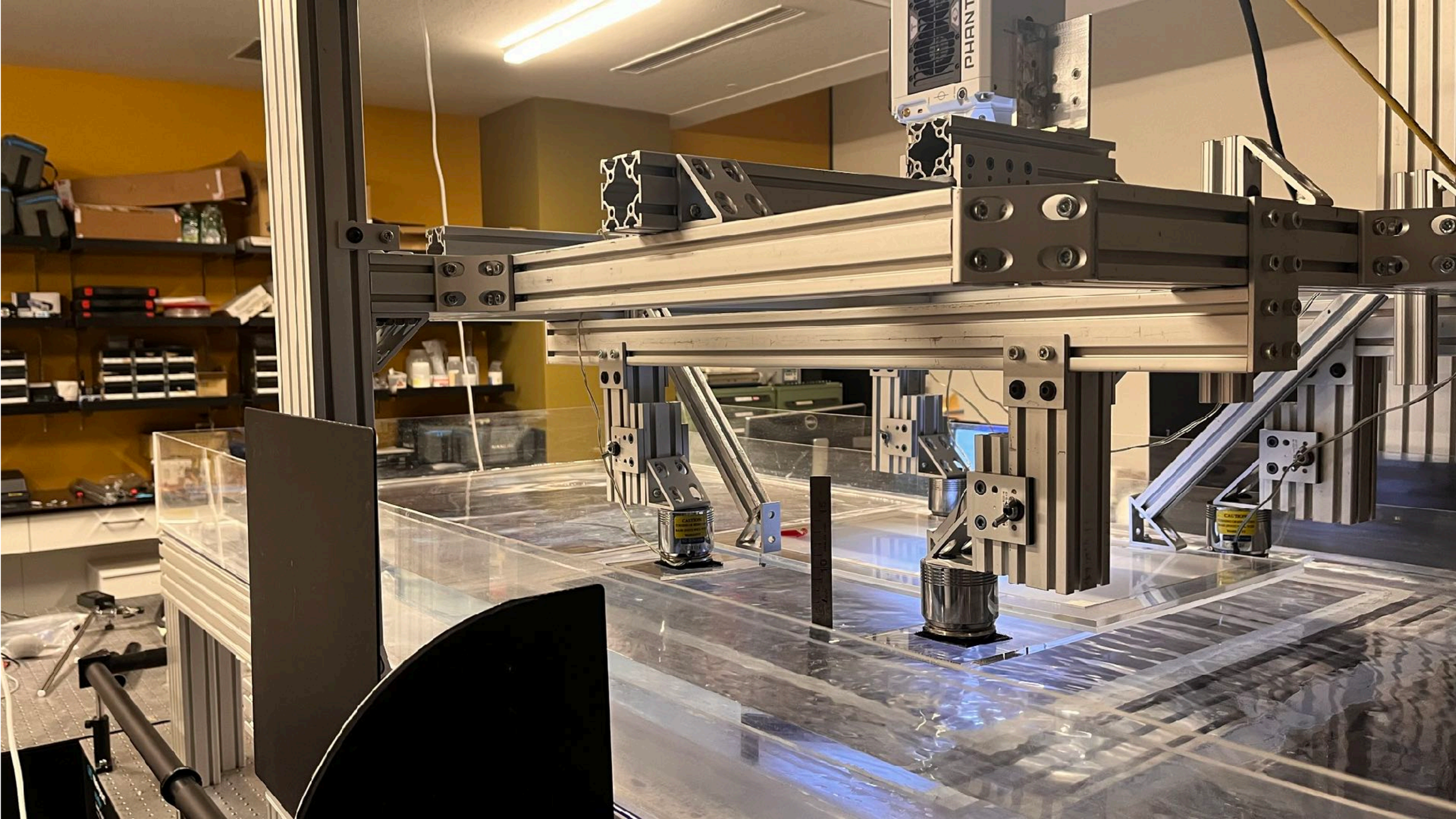
PHANTOM

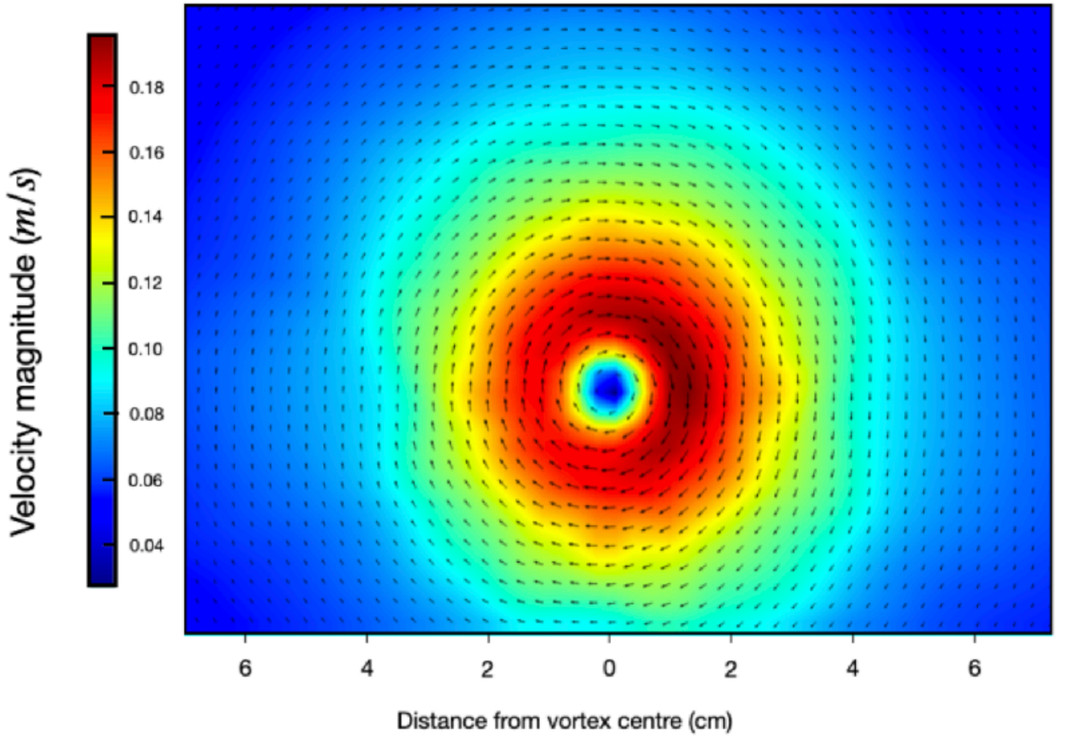
Velocity magnitude (m/s)
0.18
0.16
0.14
0.12
0.10
0.08
0.06
0.04
6
4
2
0
2
4
6
Distance from vortex centre (cm)

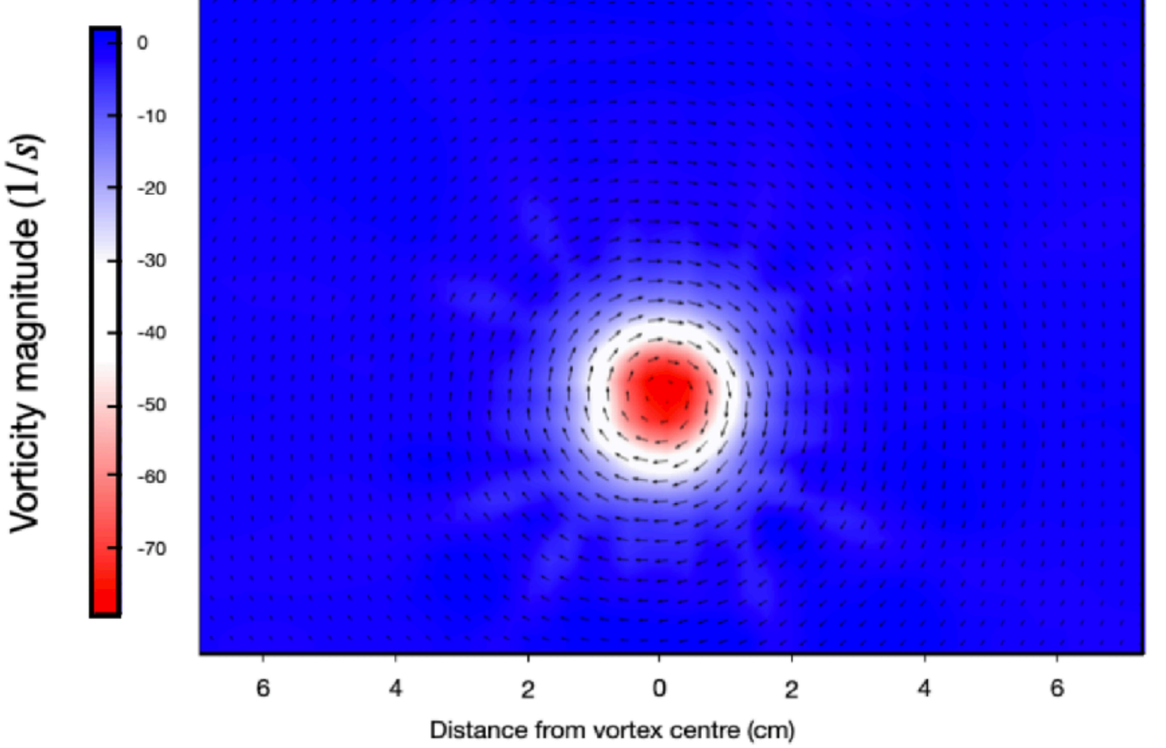
Vorticity magnitude (1/s)
0
-10
-20
-30
-40
-50
-60
-70
6
4
2
0
2
4
6
Distance from vortex centre (cm)

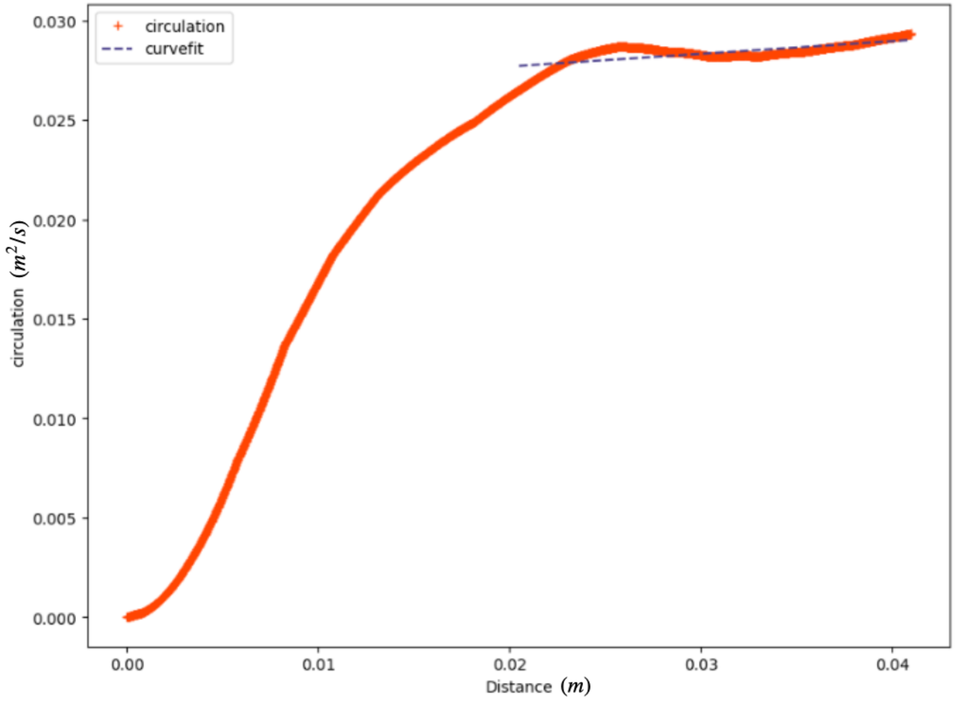
circulation
curvefit
circulation (m²/s)
0.030
0.025
0.020
0.015
0.010
0.005
0.000
0.00
0.01
0.02
0.03
0.04
Distance (m)

Requirements and Systematics

- AB effect applies under adiabatic transport conditions: **A** & **U** are small & vary slowly relative to propagating wave.
- Waves generated by acoustic transducers in the experiment have **U**/c << 1 (~ 0.001 in experiments).
- Hk << 1 (~0.04 in experiments).
- Vortex core radius ~ 0.5 cm, minimum wavelength selected in experiments ~ 2.25 cm.
- Waves also travel from transducer plates outwards to tank walls and reflect back. Experiment is performed in the duration before the reflected waves interfere with the interrogation area (approx. 1.8 seconds).
- Group velocity defined for traveling waves; measured before experiment with traveling waves from single transducer.
- We will setup ramps along tank walls within the water column to dampen wave reflections in future.

Results

$$\alpha = -0.51$$

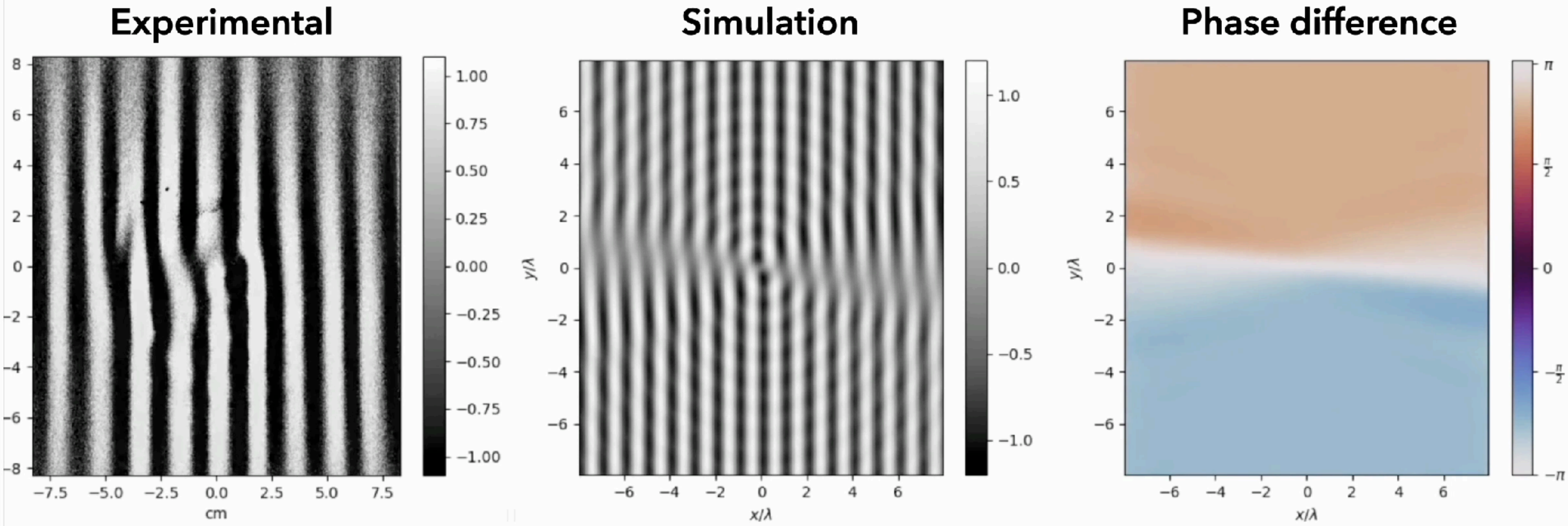

System spanning nodal lines radiate out into far field and rotate in opposite sense to the vortex.

They disappear and re-appear around horizontal axis (x-axis).

Results

$$\alpha = -0.93$$

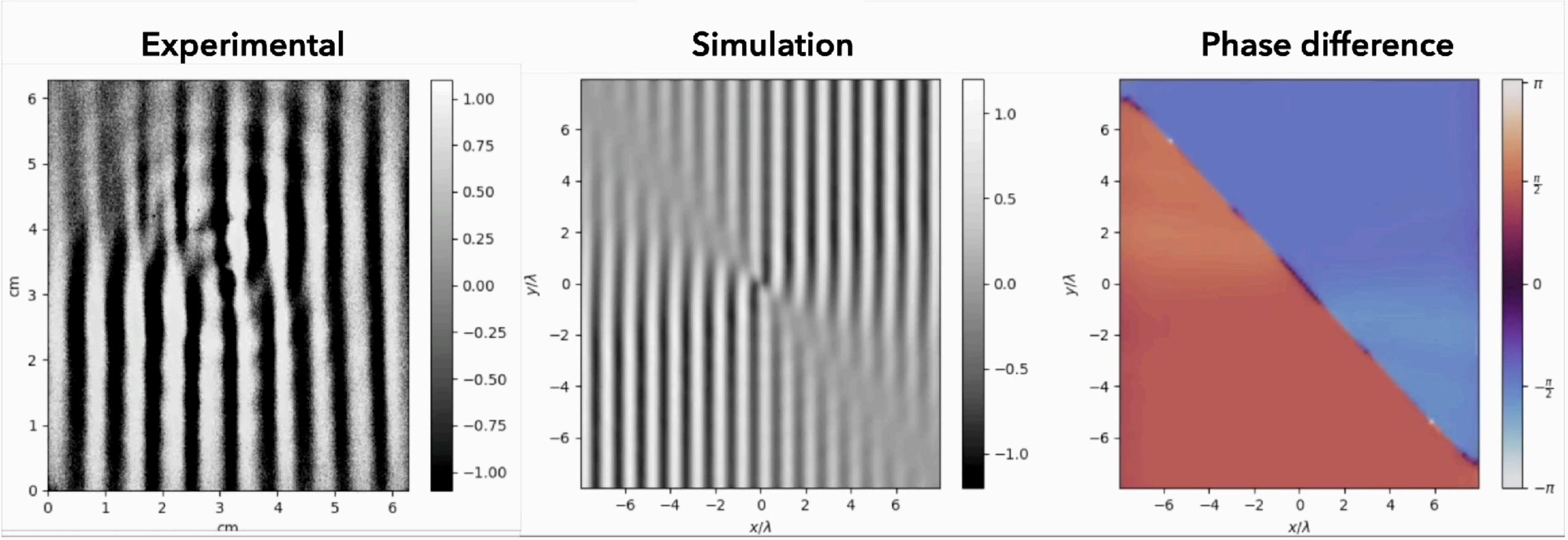

The disappearance and re-appearance (temporal oscillations) cease when $|\alpha|$ crosses an integer value.

$$\alpha = -1.04$$

Experimental

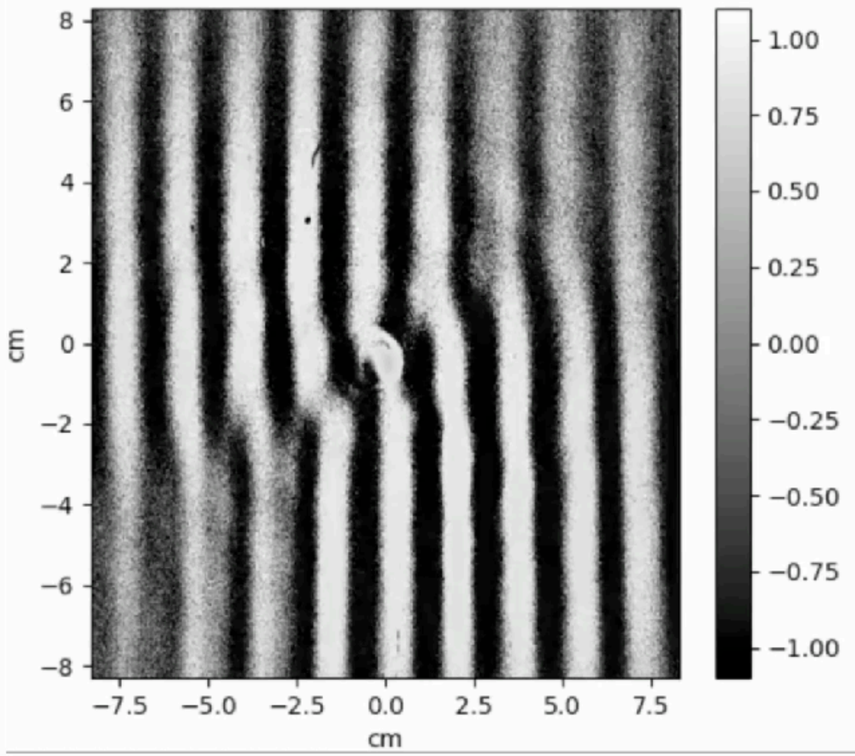

Simulation

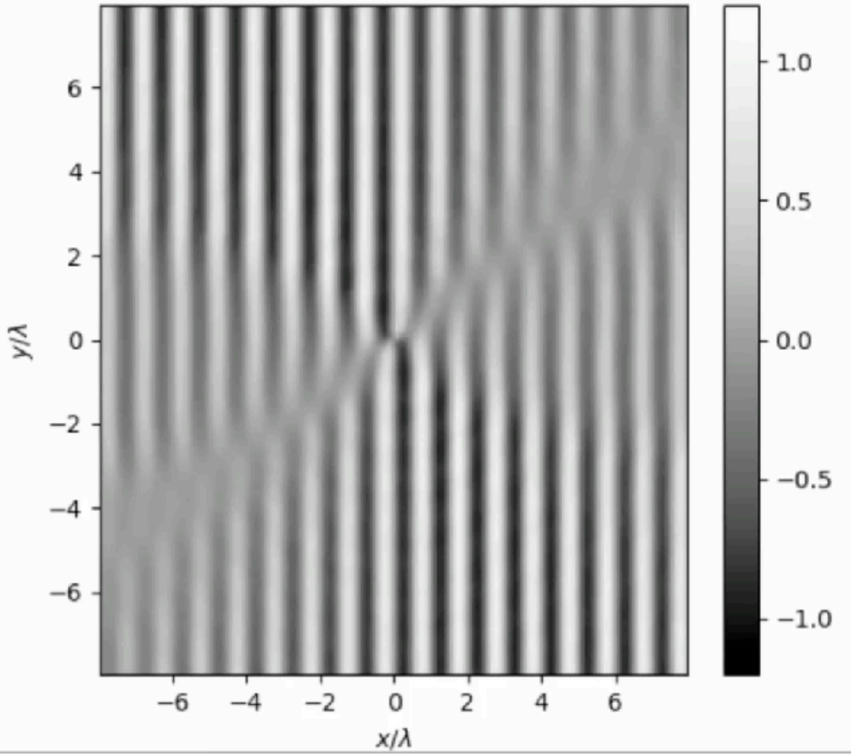

Phase difference

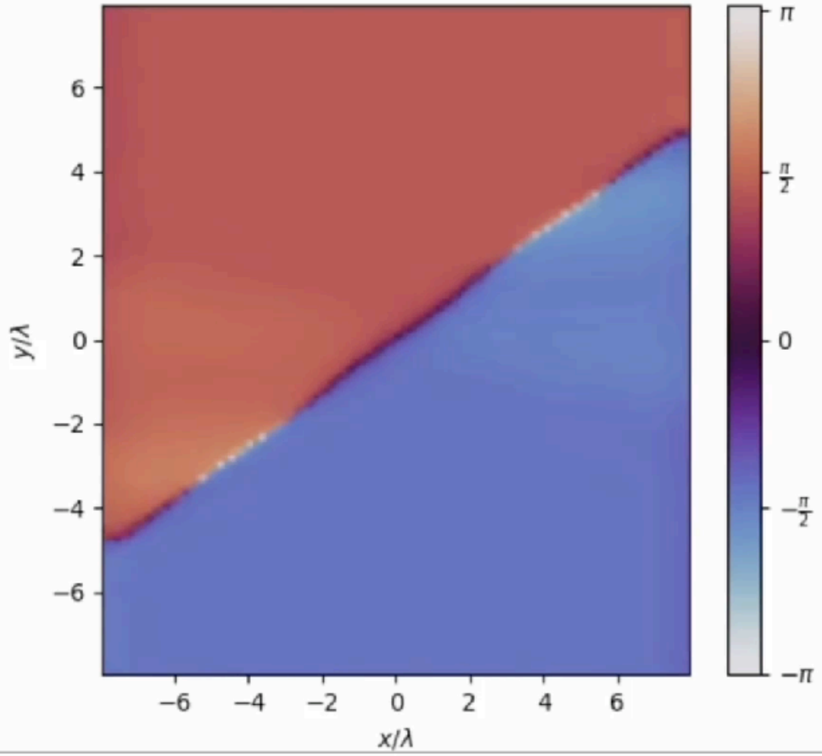

$\alpha = -2.5$

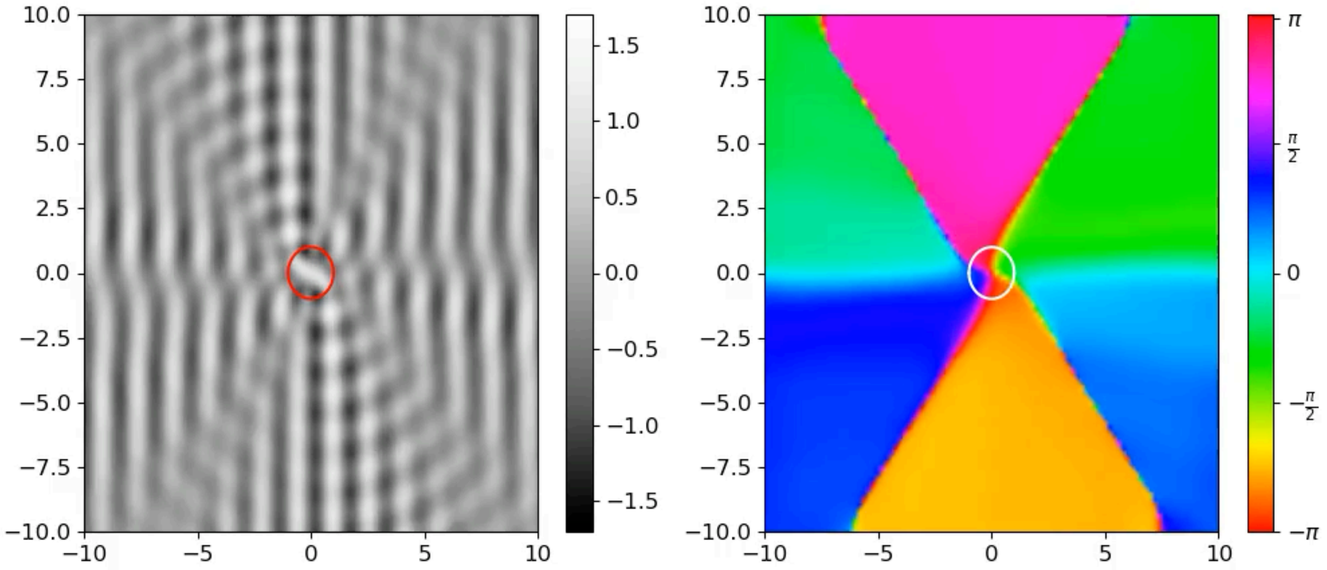

$\alpha = -3$

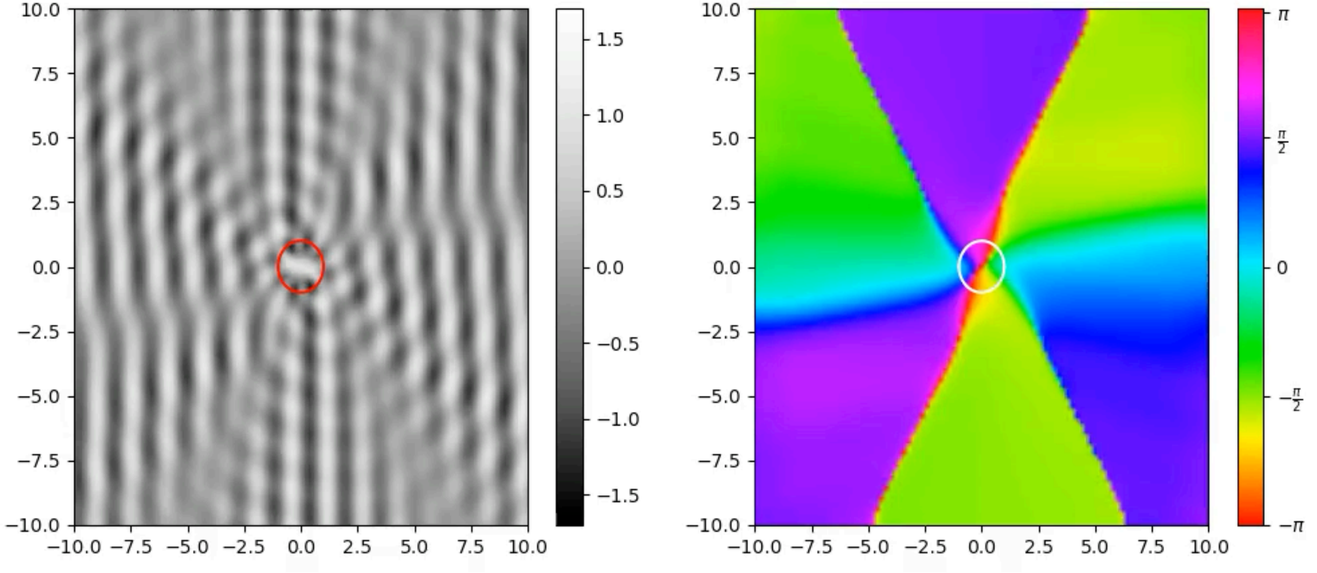

Nodal lines agree with asymptotic solution of ψ & $\eta(r, \varphi, t)$ away from x-axis using polar coordinates (r, φ):

$$\eta \sim \begin{cases} \cos\left(\alpha\varphi - \nu t - \alpha\frac{\pi}{2}\right)\cos\left(kr\cos\varphi - \alpha\frac{\pi}{2}\right), & \varphi \in (0, \pi) \\ \cos\left(\alpha\varphi - \nu t + \alpha\frac{\pi}{2}\right)\cos\left(kr\cos\varphi + \alpha\frac{\pi}{2}\right), & \varphi \in (-\pi, 0) \end{cases}$$

Nodal lines defined by zeros of time-dependent cosine function: $\alpha\varphi - \nu t - \alpha\frac{\pi}{2}\text{sgn}(\varphi) = m\pi + \frac{\pi}{2}; \quad m \in \mathbb{Z}$

Nodal lines' angular coordinate depends on α & changes linearly in t: $\theta(t) = \frac{m\pi}{\alpha} - \frac{\pi}{2\alpha} + \frac{\nu t}{\alpha} + \frac{\pi}{2}\text{sgn}(\theta)$

No. of nodal lines quantized by α & oscillate between nearest integers for non-integer values.

Branch solution describes same lines passing through origin and into the two half planes.

Nodal lines rotate at constant rate $\omega = \nu/\alpha$. Thus, direction determined by sign of α & opp. of vortex circulation.

Regions separated by nodal lines out of phase as 1st factor changes sign on nodal lines; phase shift of π.

Separation of nodal lines is approximately $\Delta\theta \approx \pi$.

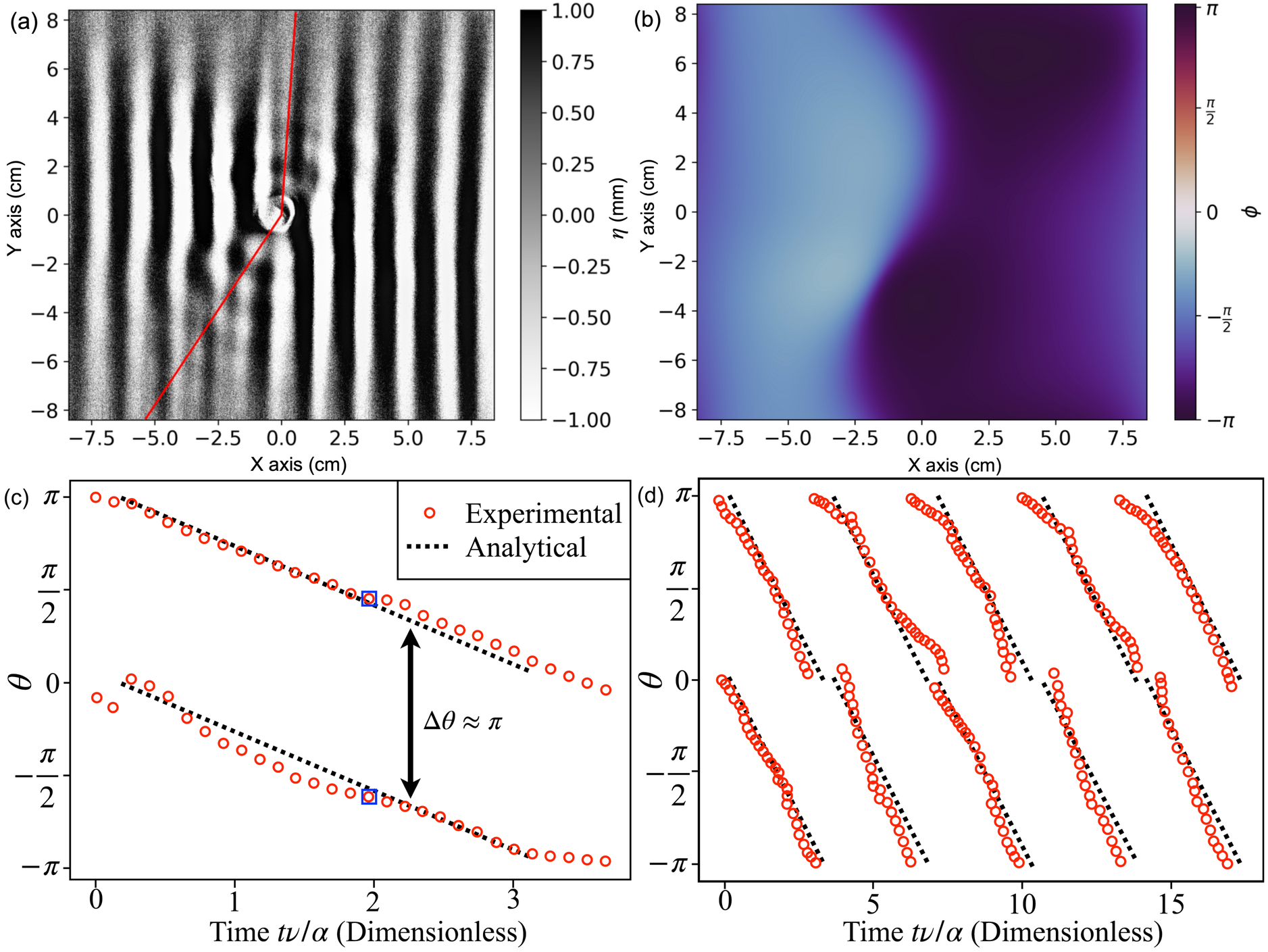
(a)
Y axis (cm)
X axis (cm)
η (mm)
(b)
Y axis (cm)
X axis (cm)
ϕ
(c)
Experimental
Analytical
Δθ ≈ π
θ
Time tν/α (Dimensionless)
(d)
θ
Time tν/α (Dimensionless)

Both quantum & fluid systems have same asymptotes after neglecting terms of $\mathcal{O}(kr)^{-1/2}$ representing scattered wave.

Prior works showed wave function of scattered plane wave had dislocation in wave fronts.

In standing waves, this is replaced by rotating nodal lines radiating from vortex separating regions of different phases.

Since ψ analogous to time-independent η_0, we include time-dep. via factor $e^{-i\nu t}$ & take real part to get η.

Asymptotic away from x-axis: $$\eta \sim \begin{cases} \cos[-kr\cos(\varphi) + \alpha\varphi - \nu t] + \cos[kr\cos(\varphi) + \alpha(\varphi - \pi) - \nu t], & \varphi \in (0, \pi) \\ \cos[-kr\cos(\varphi) + \alpha\varphi - \nu t] + \cos[kr\cos(\varphi) + \alpha(\varphi + \pi) - \nu t], & \varphi \in (-\pi, 0) \end{cases}$$

This can be re-expressed as $$\eta(r, \varphi, t) \sim \begin{cases} \cos\left[\alpha\varphi - \nu t - \alpha\frac{\pi}{2}\right] \cos\left(kr\cos\varphi - \frac{\alpha\pi}{2}\right), & \varphi \in (0, \pi) \\ \cos\left[\alpha\varphi - \nu t + \alpha\frac{\pi}{2}\right] \cos\left(kr\cos\varphi + \frac{\alpha\pi}{2})\right), & \varphi \in (-\pi, 0) \end{cases}$$

Nodal lines determined from zeros of 1st factor: $$\theta_m = \begin{cases} \frac{m\pi}{\alpha} - \frac{\pi}{2\alpha} + \frac{\pi}{2} + \frac{\nu t}{\alpha} & 0 < \theta_m < \pi \\ \frac{m\pi}{\alpha} - \frac{\pi}{2\alpha} - \frac{\pi}{2} + \frac{\nu t}{\alpha} & -\pi < \theta_m < 0 \end{cases}$$

We will now study this equation at t = 0, examining the structure of Re(ψ).

$\alpha < 1$: No zeros in the domain

$\alpha = 1$: zero just outside at $\theta = 0$ & π, coinciding with $\eta(\varphi \in 0; \pi, t = 0) = 0$.

$\alpha = 1 + \epsilon$ $(\epsilon \ll 1)$, 0 for $\alpha = 1$"splits" & moves into upper half plane as 2 lines at $\theta = \epsilon\pi/2$ & $\theta = \pi - \epsilon\pi/2$.

Distance between lines decreases as ϵ increases, at $\alpha = 2$, we get $\theta = \pi/4$ & $\theta = 3\pi/4$.

This is the structure at t = 0.

Now let's add time-dependence.

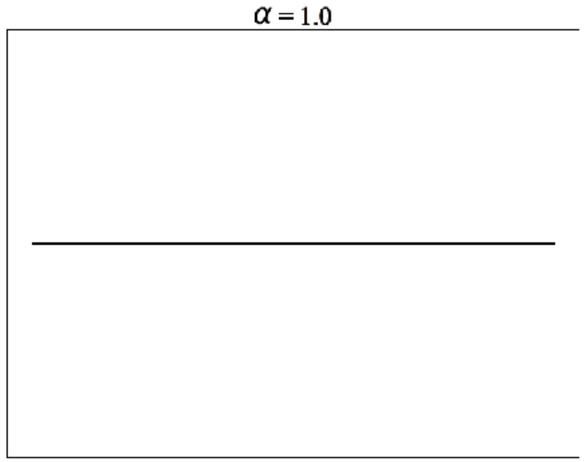

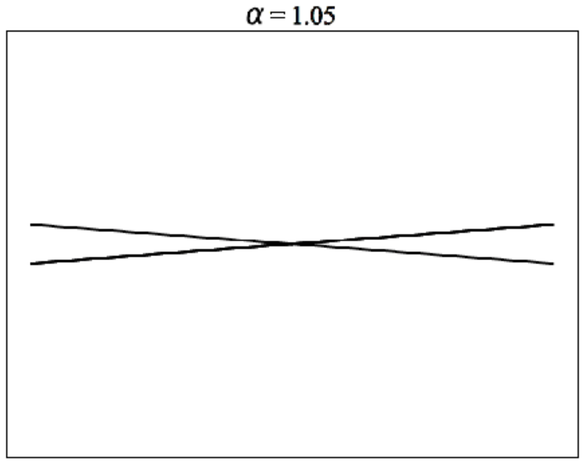

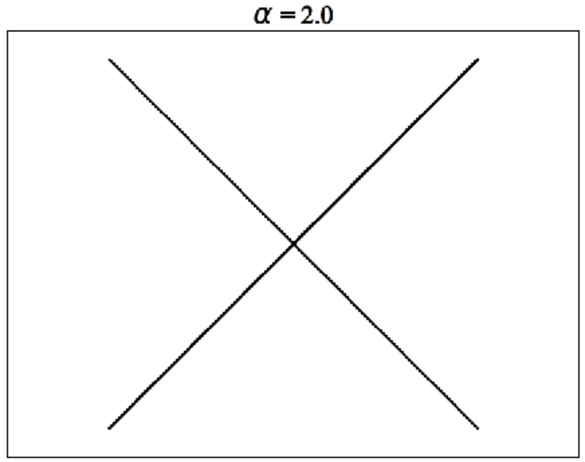

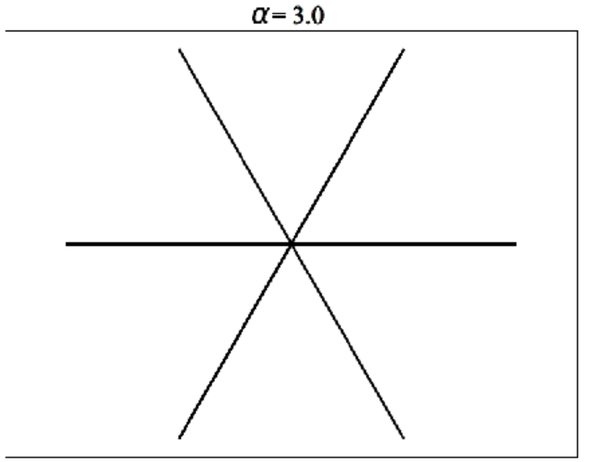

With $t \neq 0$, nodal lines rotate in direction opp. of the current. Time-dependence makes nodal lines appear & disappear.

This is captured through asymptotic at $\varphi = 0 \ \& \ \pi$:

$$\eta(r, \varphi \in \{0, \pi\}, t) \sim \cos(kr)\cos(\nu t)[1 + \cos(\pi\alpha)] - \sin(kr)\sin(\nu t)(1 - \cos(\pi\alpha))$$

$\sin(\nu t) \ \& \ \cos(\nu t)$ are linearly independent; expression = 0 only when α is an integer.

Ergo, when α is non-integer, nodal lines must disappear temporarily when approaching the x-axis.

Far-field doesn't capture region of width $\Delta\varphi \sim \mathcal{O}(kr)^{-1/2}$ near x-axis, so disappearance mechanism can't be explained.

In animations, we do see nodal lines disappear by colliding with another line created inside uncaptured region.

Also notice for $\lfloor\alpha\rfloor$ even, there's no zero outside domain at t = 0, which will enter it as time increases. To see this consider $\alpha = 2N(1 + \epsilon)$ with $(\epsilon \ll 1)$ & N positive integer. This has zeros:

$$\theta_m = \frac{2N + 2m - 1}{4N}\pi + \frac{1 - 2m}{4N}\epsilon\pi + \frac{\nu t}{2N}$$

At t = 0, this has 2N zeros $(m = -N + 1 \ldots m = N)$ but for $\nu t = \pi/2$, 2N+1 zeros $(m = -N \ldots m = +N)$

Ergo, no. of nodal lines oscillate between $\lfloor\alpha\rfloor \ \& \ \lceil\alpha\rceil$.

Summary, so far…

- Standing waves interacting with a vortex exhibit system spanning, rotating nodal lines.
- Nodal lines classically quantized for integer α values & oscillate for non-integer values.
- Nodal lines rotate in opposite sense to vortex circulation.
- Phase observable classically but not in quantum, which we exploit in our experiments and analysis.
- Nodal lines should still be unobservable; wave function's time dependence does not show up in $|\psi|^2$.
- Story not yet complete, few comments follow…

Singh et al *Communications Physics* **9**, 123 (2026)

Interpretation 2: Frame Dragging.

- Ripples in standing water obey the Eq.: $\frac{1}{c^2}\partial_t^2\eta = \nabla^2\eta;\ \ c^2 = gh\,.$
- If water flowing with velocity ***U***(x, t): $\frac{1}{c^2}\left(\partial_t + \vec{U}\cdot\vec{\nabla}\right)^2\eta = \nabla^2\eta = \frac{\partial^2\eta}{\partial r^2} + \frac{1}{r^2}\frac{\partial^2\eta}{\partial\varphi^2}.$
- Assume ***U*** varies over several λ and re-interpret as Klein-Gordon (KG) Eq. in (2+1)D curved space-time.
- KG Eq. \w metric: $ds^2 = (c^2 - U^2)dt^2 + 2\frac{\Gamma}{2\pi}d\varphi dt - r^2d\varphi^2 - dr^2$ exactly same as Eq. governing waves in tank with background flow (from vortex). Assume U << c & working to 1st order in velocity
- Metric re-written as $ds^2 = c^2\left(dt + \frac{\Gamma}{2\pi c^2}d\varphi\right)^2 - dr^2 - r^2d\varphi^2.$

- Change coordinates to $\{\tau, \varphi, r\}$ where $\tau = t + a\varphi;\ \ a = \dfrac{\Gamma}{2\pi c^2}$ & bring metric to the form

- $ds^2 = c^2(dt^2) - dr^2 - r^2 d\varphi^2$. Wave Eq. now has "flat space" metric: $\dfrac{1}{c^2}\dfrac{\partial^2 \eta}{\partial \tau^2} = \dfrac{\partial^2 \eta}{\partial r^2} + r^{-2}\dfrac{\partial^2 \eta}{\partial \varphi^2}.$

- Assume separable form $\xi(\tau, \varphi, r) = T(\tau)\Phi(\varphi)R(r)$: $T(\tau) \propto e^{-i\nu\tau};\ \ \Phi(\varphi) \propto e^{i\lambda\varphi}$ and R(r) satisfies Bessel's equation of fractional order $\dfrac{d^2R}{dr^2} + \dfrac{1}{r}\dfrac{dR}{dr} = \left(\nu^2 - \dfrac{\lambda^2}{r^2}\right)R = 0.$

- Soln. linear combination of func.: $\xi_{\nu,\lambda}(\tau, \varphi, r) = \text{Re}\left[J_\lambda(\nu r)e^{-i\nu\tau}e^{i\lambda\varphi}\right]$; J_λ: Bessel func. of 1st kind of order λ.
- In lab frame, we get $\xi_{\nu,\lambda}(t, \varphi, r) = \text{Re}\left[J_\lambda(\nu r)e^{-i\nu(t-a\alpha)}e^{i\lambda\varphi}\right]$.
- Single-valuedness of solution in φ requires: $e^{i(\nu a-\lambda)2\pi} = 1 \Rightarrow \nu a - \lambda = l$ must be integer.
- Ergo, the pattern (nodal lines) rotate with frequency ν/α.

- Lense-Thirring: subtle GR effect concerning determination of inertial frames.
- Newtonian Gravitational potential is small (~ 10^{-10} for Earth, ~10^{-6} for the Sun in natural units).
- LT yet smaller by factor β, typical speed of matter in light speed units (e.g. rot. speed of point on equator).

J Lense & H Thirring, *Physikalische Zeitschrift* **19**, 156 (1918)

- Interpretation 1: vortex as analog to solenoid. Interpretation 2: vortex as a rotating black hole/neutron star.
- Equations mappable in both cases to the shallow water Eq. & agree with theory to linear order.

- Not serendipity: Two reasons why the experiment gives two interpretations from disparate scales of physics.
- Reason 1: A unified geometric interpretation connects AB & LT.
- In our draining bathtub vortex experiment, both effects arise from the same underlying topological structure.
- Circulation-induced time transformation generates an effective vector potential governing wave propagation.
- Places AB/LT on common footing as manifestations of a single holonomy set by the vortex circulation.

- Reason 2: Gravitoelectromagnetism predates both QM & GR: O Heaviside, *The Electrician* **1**, 455 (1893)
- The current experiment combines EM in AB and GR with fluids.

Comparison of GEM and Maxwell's equations

Law	GEM equations	Maxwell's equations
Gauss's law	$\nabla \cdot \mathbf{E}_\mathrm{g} = -4\pi G\rho_\mathrm{g}$	$\nabla \cdot \mathbf{E} = \frac{\rho}{\varepsilon_0}$
Gauss's law for magnetism	$\nabla \cdot \mathbf{B}_\mathrm{g} = 0$	$\nabla \cdot \mathbf{B} = 0$
Faraday's law of induction	$\nabla \times \mathbf{E}_\mathrm{g} + \frac{\partial \mathbf{B}_\mathrm{g}}{\partial t} = 0$	$\nabla \times \mathbf{E} + \frac{\partial \mathbf{B}}{\partial t} = 0$
Ampère–Maxwell law	$\nabla \times \mathbf{B}_\mathrm{g} - \frac{1}{c^2}\frac{\partial \mathbf{E}_\mathrm{g}}{\partial t} = -\frac{4\pi G}{c^2}\mathbf{J}_\mathrm{g}$	$\nabla \times \mathbf{B} - \frac{1}{c^2}\frac{\partial \mathbf{E}}{\partial t} = \frac{1}{\varepsilon_0 c^2}\mathbf{J}$

where:

- $\mathbf{E}_\mathrm{g}$ is the gravitoelectric field (conventional gravitational field), with SI unit $\mathrm{m \cdot s^{-2}}$
- $\mathbf{E}$ is the electric field, with SI unit $\mathrm{kg \cdot m \cdot s^{-3} \cdot A^{-1}}$
- $\mathbf{B}_\mathrm{g}$ is the gravitomagnetic field, with SI unit $\mathrm{s^{-1}}$
- $\mathbf{B}$ is the magnetic field, with SI unit $\mathrm{kg \cdot s^{-2} \cdot A^{-1}}$
- ρ_g is mass density, with SI unit $\mathrm{kg \cdot m^{-3}}$
- ρ is charge density, with SI unit $\mathrm{A \cdot s \cdot m^{-3}}$
- $\mathbf{J}_\mathrm{g}$ is mass current density or mass flux, with SI unit $\mathrm{kg \cdot m^{-2} \cdot s^{-1}}$
- $\mathbf{J}$ is electric current density, with SI unit $\mathrm{A \cdot m^{-2}}$
- G is the gravitational constant, with SI unit $\mathrm{m^3 \cdot kg^{-1} \cdot s^{-2}}$
- ε_0 is the vacuum permittivity, with SI unit $\mathrm{kg^{-1} \cdot m^{-3} \cdot s^4 \cdot A^2}$
- c is both the speed of propagation of gravity and the speed of light, with SI unit $\mathrm{m \cdot s^{-1}}$.

Acknowledgements

- Discussions with R Govindarajan, D Levine, A Saxena, D Mitra & CP Connaughton.
- J Featherstone and K Bauer for scientific visualization of experimental schematics.
- MMB thanks ICTS, Bengaluru for hosting while writing final parts of the manuscript.
- Funded by OIST through subsidy funding from the Cabinet Office of the Prime Minister of Japan.

Singh et al *arXiv: 2604.21543* (2026) (In Review)

Thank You

Email: bandi@oist.jp